

Experimental study of amorphous silicate formation

S. Wada¹, Y. Murata¹, A. T. Tokunaga², and J. Watanabe¹

¹ Department of Applied Physics and Chemistry, The University of Electro-Communications, Chofugaoka, Chofu, Tokyo 182-8585, Japan

² Institute for Astronomy, University of Hawaii, 2680 Woodlawn Dr., Honolulu, HI 96822, USA

Received 29 January 2003 / Accepted 13 May 2003

Abstract. Broad infrared bands at 10 and 18 μm have often been observed around oxygen-rich evolved stars, and these are thought to arise from amorphous silicate dust grains. In order to study the formation mechanism of silicate dust grains, we have analyzed synthesized silicate dust analogs by reflection absorption infrared spectroscopy (RAIRS) and X-ray photoelectron spectroscopy (XPS). The dust analog was produced from SiO and Mg vapors in O₂. The analyses showed that an amorphous silicate is formed at about temperature of 650 K through O-deficient silicate formation. However, when the substrate temperature was below 650 K, the main product is a mixture of SiO_x and MgO, where $1 < x \leq 2$. Our experimental results indicate that temperature is an important factor for amorphous silicate formation in the circumstellar environment of oxygen-rich evolved stars.

Key words. ISM: dust, extinction – circumstellar matter – stars: mass loss – methods: laboratory

1. Introduction

Oxygen-rich evolved stars form silicate/metal oxide dust grains in a course of their mass loss process. Broad 10 and 18 μm peaks observed in emission or absorption have been attributed to an amorphous silicate. Well-known amorphous silicates are a type of glass. Glass is a quenched liquid with silica rich composition in which SiO₂ is more abundant than MgO and FeO. Amorphous olivines and amorphous pyroxenes whose compositions are 2(MgO+FeO)+SiO₂ and (MgO+FeO)+SiO₂ respectively have been proposed as candidate materials of amorphous silicate dust grains around oxygen-rich evolved stars. However, it is very difficult to make a glass whose composition is rich in MgO + FeO like an olivine. Dorschner et al. (1995) produced amorphous/glassy silicate from melts by a very rapid cooling method.

Various methods have been used to synthesize silicate dust analogs with an infrared spectrum resembling that of the interstellar medium and circumstellar shells. These methods include arc melting of silicate (Dorschner et al. 1986), quenching of melts (Jäger et al. 1994; Dorschner et al. 1995), deposition from a gas mixture (Day 1979; Nuth & Donn 1983; Wada et al. 1991; Koike & Tsuchiyama 1992; Kaito et al. 2001), and condensation from evaporates of a laser heated silicate (Stephens & Russell 1979; Brucato et al. 1999). These authors compare the infrared band features of their materials to the interstellar band features at 10 and 18 μm . They also

compare to spectral features in the near infrared region because astronomical silicates are mixed with other dust components.

In these simulation experiments of circumstellar shells, unusual solids were often detected in condensates produced from vapors. Rietmeijer et al. (1999) synthesized condensates from a Mg-Fe-SiO-H₂-O₂ vapor and they found amorphous grains with unique mixed “MgSiO” and “FeSiO” compositions of metastable eutectics together with oxides in the condensates. Kaito et al. (2001) observed laboratory-products from Mg and SiO smoke by high-resolution transmission electron microscope. They detected amorphous MgSiO, Si crystallites, Mg, Mg₂Si, MgO, Mg₂SiO₄ crystal, and Mg₂SiO₄ and Si mixed crystal in the products.

Crystalline silicates are formed by heating of amorphous dusts after condensation. Brucato et al. (1999) determined the activation temperature for crystallization and suggested that crystalline silicates would be formed by the long term exposure of amorphous dusts to a temperature of higher than 770 K.

A dust shell develops around a mass-loss star. It is generally thought that the highest temperature of the dust in the dust forming region corresponds to the condensation temperature of dusts. Using low resolution spectra (LRS) of Infrared Astronomical Survey (IRAS), Simpson (1991) found the temperature of inner boundaries of dust shells is 400–800 K. This temperature is too low to form crystalline silicate in a short period of time.

In the circumstellar environment, dust grains are formed from gaseous species. Until recently, there is little experimental work concerning the formation mechanism of dusts. Our purpose is to clarify the formation process of dust by analysing the

Send offprint requests to: S. Wada,
e-mail: wada@e-one.uec.ac.jp

condensate from SiO and Mg vapors using reflection absorption infrared spectroscopy (RAIRS) and X-ray photoelectron spectroscopy (XPS).

In this paper we will attempt to address the questions of the nature of astronomical amorphous silicates and their formation mechanism by experiment and comparison to astronomical observations.

2. Experimental

Dust analogs were synthesized experimentally in the following manner. A Si wafer about 1 cm wide and 5 cm long was set in an apparatus which can be evacuated to under 10^{-3} Pa. The wafer was attached to a tantalum foil that was connected to a copper electrode. Heating of the Si wafer was achieved by applying direct current to the copper electrode.

The Si wafer was heated up to 1120–1170 K with electric power directly in an atmosphere of oxygen. An oxygen pressure of higher than about 2 Pa is required to produce SiO vapor. However, if the oxygen pressure is too high then SiO₂ forms and sticks to the surface of the Si wafer, thus preventing the formation of SiO vapor. Therefore an oxygen pressure of either 6.5 Pa or 13 Pa was used to enhance the production of SiO.

To obtain Mg vapor, thin magnesium ribbons were heated in an alumina tube with a nichrome heater. The both vapors were condensed onto a tantalum substrate set at a distance of 5 or 50 mm apart from both vapor sources. The sample MS-1 used a distance of 50 mm, while the samples MS-2 and MS-3 were collected with a distance of 5 mm.

SiO and Mg were evaporated simultaneously in an oxygen atmosphere for 15–30 min. We controlled the evaporation rate of the Si wafer by monitoring the temperature with a pyrothermometer. However, it is difficult to control the evaporation rate of magnesium because of the low vaporization temperature of Mg. When the temperature of the magnesium source was too high, the color of the products became blue-gray (Mg metal-rich), while at lower temperatures a pale white product (SiO_x-rich) was obtained.

After synthesis, we obtained the RAIRS of the products with a Spectrum 2000 (Perkin-Elmer Co.) and the XPS with a ESCA-K1 (Shimadzu Co.). RAIRS was obtained instead of an absorption spectrum because the sample was too thin to produce either a good spectrum in transmission directly or with the KBr pellet method.

3. Results and discussion

3.1. Infrared spectra

RAIRS is used for a measurement of a spectrum of a very thin film deposited on a metal substrate. In our experiments, we prepared sample films whose thickness did not produce an absorbance greater than 0.2 at the 9–10 μm peak. The thickness was approximately 100–300 nm. Note that the RAIRS spectra are essentially the same as the absorption spectra obtained by the KBr pellet method except for the reflectivity effect of the substrate metal in the case of amorphous and polycrystalline solids. The RAIRS method is described by Golden (1985).

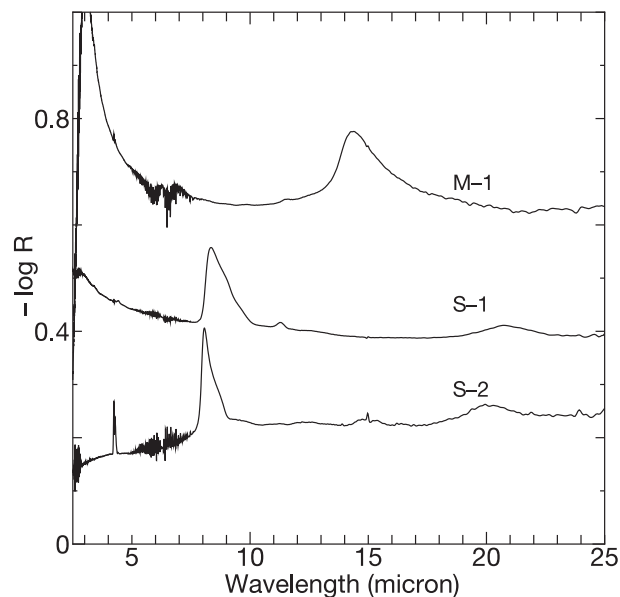


Fig. 1. RAIRS of synthetic oxides measured with an incidence angle of 60° . Vertical axis is $-\log R$, where R is the reflectance. M-1: MgO which was formed on a cold substrate from a Mg vapor in 13 Pa of ambient O₂ gas. S-1: a product which was formed on a cold substrate (about 300–330 K) from a SiO vapor in 13 Pa of ambient O₂ gas. S-2: a product which was formed on a hot substrate (~ 650 K) from a SiO vapor in 6.5 Pa of ambient O₂ gas. Sharp peaks at 4.2 μm and many fine peaks ~ 6 μm are caused by atmospheric CO₂ and H₂O, respectively.

RAIRS of samples are shown in Figs. 1 and 2. The sample S-1 is a condensate collected on the cold substrate (300–330 K), which was made from the SiO vapor only. Peaks appear at 8.2, 11.2 and 20.7 μm as shown in Fig. 1. The sample S-2 is a condensate from SiO vapor on a hot substrate at 650 K. In the spectrum, peaks are observed at 8 and 20 μm , however there is no peak in the 11–17 μm spectral region.

It is known that in the absorption spectrum of SiO₂ three TO modes give rise to absorption peaks; asymmetric stretching of O-Si-O (AS, ~ 9 μm), symmetrical stretching of the oxygen atom along a line bisecting the axis formed by the two Si atoms (SS, 12.5 μm), and rocking of the oxygen atom around the axis connecting the two silicon atoms (R, 21.5 μm). More precisely, the AS is composed of two modes. In one stretching mode neighboring oxygen atoms move in phase (AS₁, 9.30 μm) and in the other mode they move out of phase each other (AS₂, 8.70 μm) (Trchová et al. 1997).

Moreno et al. (1997) analyzed infrared spectra of a SiO₂ film of various thickness. The 9–10 μm -band feature of SiO₂ shows complicated variations depending on incidence angle and the film thickness. Therefore we prepared samples with a constant film thickness and measured RAIRS spectra with a fixed incidence angle of 60° or 75° . These angles were chosen because the best spectra were obtained at these angles; the spectra were more noisy at higher angles.

In the infrared transmission absorption spectra of solid-SiO_x ($1 < x < 2$), the AS peak usually appears at a longer wavelength than that of SiO₂. The peak moves to the shorter wavelength region with increasing concentration of oxygen

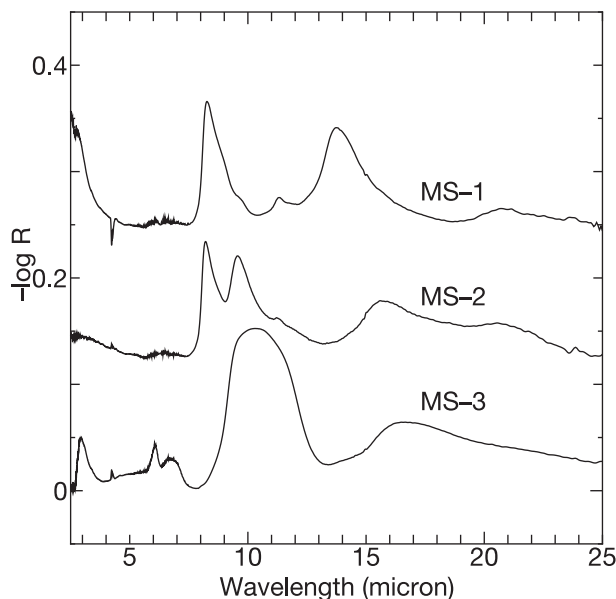


Fig. 2. RAIRS of products from Mg and SiO measured with an incidence angle of 75° (MS-1) and 60° (MS-2 and MS-3). MS-1: a product formed on a cold substrate. MS-2: a product formed on a hot (650 K) substrate. MS-3: a product formed on a hot (650 K) substrate.

(Nakamura et al. 1984). Another index for the oxygen concentration of SiO_x is the SS peak. The peak at $12.5 \mu\text{m}$ peak in SiO_2 spectrum is not observed in the SiO_x produced in vacuum, instead, a small peak appears at $11.4 \mu\text{m}$.

The sample S-2 appears to be SiO_2 from its peak wavelength, although the $12.5 \mu\text{m}$ peak is not seen in the RAIRS. On the other hand, S-1 is not oxidized enough. A $11.2 \mu\text{m}$ peak in the RAIRS of S-1 corresponds to the $11.4 \mu\text{m}$ peak of SiO_x in the transmission infrared spectrum. These results indicate that SiO_x is completely oxidized if the substrate temperature is 650 K.

In the spectrum of MgO crystal, peaks caused by LO and TO modes appear at $13.9 \mu\text{m}$ and $24.9 \mu\text{m}$, respectively (Farmer 1974). A RAIRS of MgO sample is presented in Fig. 1, M-1. The sample was produced from a vapor of Mg in a 13 Pa atmosphere of O_2 . A peak is observed at $14.3\text{--}14.7 \mu\text{m}$ (LO) in the RAIRS, however the TO peak is not observed in the wavelength region of our measurements. As mentioned above, metallic Mg is often contained in the products. This is caused by the high evaporation rate of Mg.

SiO and Mg were evaporated simultaneously and condensed on substrates with different temperatures. The sample which was formed on a cold substrate is presented in Fig. 2 (MS-1). Clearly, MS-1 is a superposed spectrum of S-1 and M-1. This means that the sample is a mixture of SiO_x and MgO.

MS-2 and MS-3 were condensed on a 650 K substrate and the spectra are presented in Fig. 2. In the spectrum of MS-2 two bands appear in $8\text{--}9.5 \mu\text{m}$. These peak wavelengths correspond to those of AS_1 and AS_2 of SiO_2 . However, the wavelength of the peak seen at $15.5 \mu\text{m}$ is longer than that of MgO. We infer that phase separation occurred in MS-2 and the structure

of MgO was modified due to a chemical reaction with SiO_x . The peaks in $8\text{--}9 \mu\text{m}$ should be affected by the reaction.

Two broad bands appear at $10 \mu\text{m}$ and $16.5\text{--}17 \mu\text{m}$ in the RAIRS of MS-3. That indicates a new material form in MS-3. This spectrum has some resemblance to spectra often observed around evolved stars.

MS-2 and MS-3 were synthesized under the same experimental condition. In spectra of samples produced about $520\text{--}570 \text{ K}$, a peak around $15.5 \mu\text{m}$ appeared with or without the $\sim 14 \mu\text{m}$ –MgO band and a modified $9 \mu\text{m}$ peak was often observed. This means that a chemical reaction begins to occur in this temperature range. The temperature dependence of the reaction is a future problem.

In the next section we discuss the nature of the composition differences between MS-2 and MS-3. A temperature of about 650 K or higher was found to be necessary temperature to form silicate material.

Small peaks in the MS-3 are caused by absorption of H_2O ($3 \mu\text{m}$ and $6 \mu\text{m}$) in the air. A peak at $7 \mu\text{m}$ is often observed in spectra of Mg-containing sample, and this is caused from carbonate absorption which is produced by a reaction with CO_2 in air.

It should be noted that the RAIRS spectra shown in Figs. 1 and 2 cannot be directly compared to absorption spectra because the RAIRS spectra depend critically on the incidence angle.

3.2. X-ray photoelectron spectroscopy

XPS measures energy of the photoelectron ejected from atoms upon irradiation by X-rays. From XPS we can obtain information about the chemical bonding of the element in the material. In our XPS experiments we used $\text{MgK}\alpha$ as source of the excitation. The C 1s peak of carbon was used as an internal reference peak. We corrected the observed binding energies by using the C 1s peak (284.4 eV) which was contained in our samples as a contaminant.

Guittet et al. (2001) discussed the binding energy of Si 2p and O 1s in mixed oxides. They calculated the Si 2p-binding energy in mixed oxides using a linear combination of charge of silicon atom, the Madelung energy (Coulomb force and structure of oxides), and the relaxation energy (final state after electron emission). Their calculation agreed well with their experimental values of a crystalline olivine, ZrSiO_4 (101.8 eV) and SiO_2 (103.4 eV). The binding energy of silicon (Si) and that of a silicide (Mg_2Si) are expected to be lower than these values because of the charge of silicon atom. The binding energies are reported as 99.7 eV for silicon (Trchová et al. 1997) and 98.5 eV for silicide (An et al. 1995).

Since SiO_x ($1 < x \leq 2$) are very important materials for industrial applications, many XPS studies have been performed. The Si 2p peak of the low oxidation state appears in the lower energy region than that of SiO_2 . The difference of binding energy of Si(IV), Si(III), Si(II), Si(I), and Si(0), in which IV, III, II, I, 0 is the oxidation number of silicon, was reported to be about 1 eV by Barranco et al. (2001). In particular they reported the binding energies to be Si(IV): 103 eV , Si(III): 102 eV ,

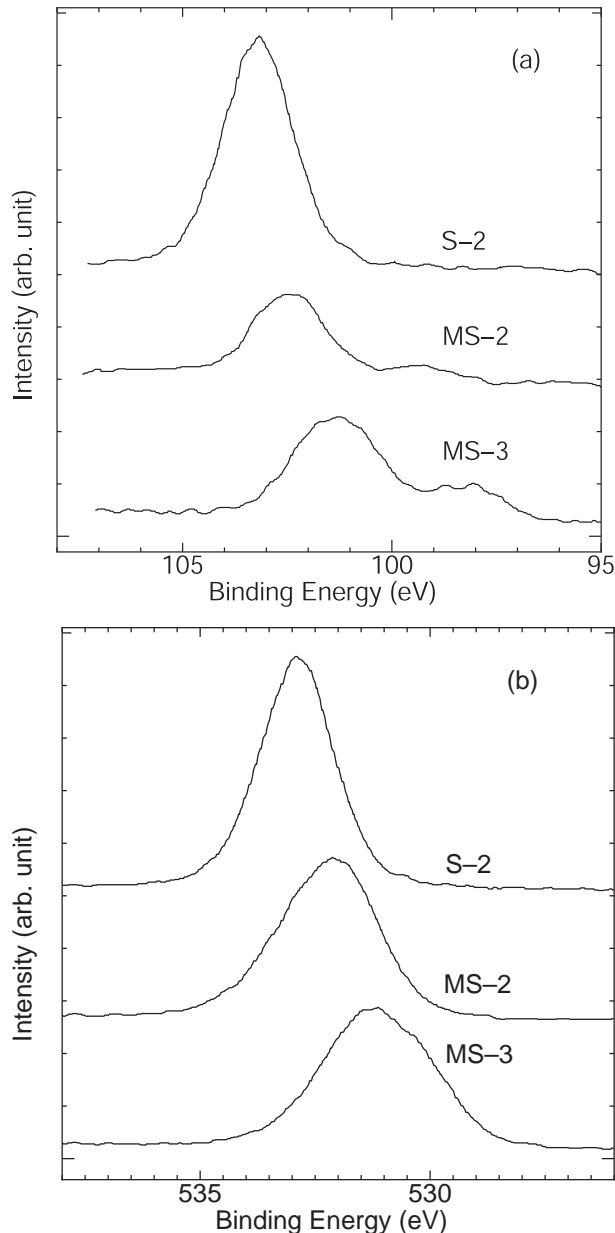


Fig. 3. a) XPS spectra of Si 2p of S-2, MS-2, and MS-3. b) XPS spectra of O 1s of S-2, MS-2, and MS-3.

Si(II):101 eV, Si(I):100 eV, Si(0): 99 eV. Barranco et al. (2001) made a condensate from SiO vapor in ultra high vacuum. The composition was $\text{SiO}_{1.3}$ and it was composed of Si(I) and Si(III) as a result of oxidation-reduction reaction of SiO.

Figure 3a shows Si 2p spectra of XPS for samples of S-2, MS-2, and MS-3. Only one peak appears at 103.2 eV in S-2. The feature is smooth and symmetrical. The peak of S-2 coincides with the binding energy of SiO_2 (103 eV). The result agrees with RAIRS measurement.

Two peaks are detected in MS-3. The main peak is found at 101.3 eV and a broad small peak is found at 98.0 eV. The peak of an olivine, ZrSiO_4 presented by Guittet et al. (2001) is very close to the 101 eV peak. However the peak of MS-3 is located on the lower energy side. We tentatively assign MS-3

to an O-deficient silicate. The peak at 98.0 eV coincides with the silicide peak.

MS-2 shows a maximum at 102.5 eV with a shoulder at 103.2 eV. The shoulder at 103.2 eV indicates the presence of SiO_2 . The peak of the MS-2 occurs at higher energy than that of MS-3. We think that the material and the peak at 99.0 eV corresponds to the peak of Si(0).

Full width at half maximum (FWHM) of peaks depends on the variety of the chemical bonds of Si. The FWHM of the main peak of S-2, MS-2, and MS-3 is 1.9, 2.1, and 2.5 eV, respectively. This indicates that there are more kinds of Si bonds in MS-3 than S-2 and MS-2.

Guittet et al. (2001) reported that binding energies of O 1s are 532.7 eV (SiO_2) and 531.3 eV (ZrSiO_4), respectively. The binding energies of oxygen shown in Fig. 3b are measured at 532.9 (S-2), 532.1 (MS-2), and 531.1 eV (MS-3). The values of full width at half maximum are 1.9 (S-2), 2.5 (MS-2), and 2.9 eV (MS-3). The binding energy is also matched with SiO_2 (S-2). The peak of MS-3 is composed of two peaks at least. Apparently, the binding energy at the maximum of the peak in MS-3 is very close to that of olivine. The O 1s-peak of MS-2 is also an intermediate value between S-2 and MS-3.

Note that the oxidation numbers of silicon atom are II in SiO molecule, and 0 in solid silicon and silicide, Mg_2Si . The presence of solid silicon and silicide appearing in MS-2 and MS-3 means that silicon atom is reduced from II to 0. On the other hand, the oxidation number of silicon atom is IV in SiO_2 and silicates. The presence of these compounds means that silicon atom is oxidized from II to IV. In other words, reactions of oxidation and reduction of silicon atoms occurred in our samples.

We performed a depth analysis of Si 2p of MS-3. The binding energy of the main peak seems to be slightly shifted to higher energy side. The peak intensity of silicide decreases with depth, as shown in Fig. 4. Most likely we are observing that the material changes to silicate as we go deeper into the sample.

3.3. Silicate formation

Based on the preceding analysis, we present the following mechanism for the formation of MS-3, as compared with that of MS-2. RAIRS of MS-3 shown in Fig. 2 is similar to emission and absorption spectra of amorphous silicate dusts around oxygen-rich evolved stars. The product of MS-3 is an amorphous silicate, since the $10 \mu\text{m}$ feature of RAIRS corresponding to asymmetric stretching of O-Si-O is broad and the wavelength is shifted to the longer side than that of SiO_2 .

Both samples of MS-2 and MS-3 were produced with the same experimental conditions with a substrate temperature of 650 K. In MS-3, the deposit reacted rapidly to form O-deficient amorphous silicates, $\text{Mg}_2\text{SiO}_{4-x}$ or MgSiO_{3-x} ($x \geq 0$) (we don't know the ratio of Mg/Si in the samples). At the same time, a small amount of reduced silicon (Mg_2Si and Si) is also produced. As mentioned above, MS-2 is a mixture of SiO_2 , SiO_x , a product reacted from SiO-MgO and silicon. It is thought that gases of Mg and SiO were not mixed

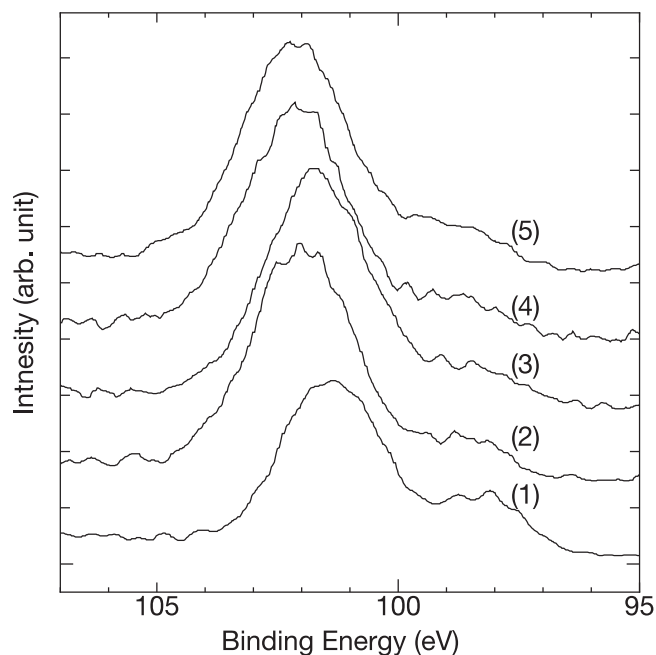


Fig. 4. Variation of XPS spectra of Si 2p with depth. Total minutes for milling by Ar ions are (1) 0 min (surface), (2) 4 min, (3) 8 min, (4) 12 min, and (5) 16 min.

well and/or the ambient O_2 pressure was slightly higher than in the experimental conditions of MS-3.

The formation of MS-3 starts from O-deficient silicates, i.e. Mg_2SiO_{4-x} or $MgSiO_{3-x}$ ($x > 0$), containing many oxygen vacancies. The structure of the O-deficient silicates is amorphous due to the O vacancies. The O-deficient silicates are considered to be less stable than completely oxidized silicates, such as Mg_2SiO_4 and $MgSiO_3$.

The O-deficient silicate, for examples, Mg_2SiO_{4-x} is more unstable than $Mg_2SiO_{4-x'}$ for $x > x'$. Thus, when the second layer of Mg_2SiO_{4-x} is formed on the first layer, a small amount of O atoms is transferred from the overlayer to the underlayer and a part of vacancies in the underlayer is occupied by O atoms. Next, the third layer is deposited and O atoms migrate from the second and the third layer to the first and the second layer, respectively. Further processes continue and the oxygen migration to the adjacent underlayer always occurs in every layer for each step.

Then, the x value of Mg_2SiO_{4-x} and $MgSiO_{3-x}$ decreases with depth and silicide of Mg_2Si and silicon is formed near the surface. This formation mechanism of MS-3 is supported by variation of XPS spectra of Si 2p with depth shown in Fig. 4. In addition to the decrease of the peak intensity corresponding to Mg_2Si with depth, the binding energy of the main peak is slightly shifted to higher binding energy side. That is, Si atoms are more oxidized with depth due to the O atom migration. The substrate temperature of 650 K is necessary for the O atom diffusion to the adjacent underlayer. As a result, silicate forms as an end member of oxidized product and silicide or silicon forms as an end member of reduced product.

After receiving O atoms from the overlayer, however, the amorphous structure is not transformed to the crystalline state,

because of the registration of the amorphous structure due to the overlayer. Thus, the underlayer silicates keep their amorphous structure.

3.4. Astronomical implications

Broad 10 and 18 μm bands have been observed in emission and absorption around oxygen-rich evolved stars. Both bands are usually attributed to amorphous silicate dusts. Various features were noted in the 8–14 μm spectral range by Little-Marenin & Little (1990), and they classified them into groups (7 groups for M Mira variables), 6 groups for oxygen-rich AGB stars, and 6 groups for red giants (Speck et al. 2000). About 32% of the M Mira variables show the standard silicate feature (denoted as “Sil” by Little-Marenin & Little 1990). The Sil feature extends from about 8–14 μm with a peak at $9.8 \pm 0.2 \mu m$. They reported a broad 18 micron peak that is often but not always observed with the Sil bands.

In some groups, a 11 μm and a 13 μm bands are observed in addition to the 10 μm peak. The $\sim 12 \mu m$ peak in M Mira variables has been attributed to alumina grain (Onaka et al. 1989). Though the 11 μm peak have been attributed to crystalline silicate (olivine; Little-Marenin & Little 1990), recently amorphous alumina grains was proposed as the candidate material for the broad 11 μm peak (Miyata et al. 2000; Begemann et al. 1997). On the other hand, a spinel which is a double oxide of aluminum and magnesium was proposed as the carrier of the 13 μm band (Fabian et al. 2001).

Another oxide, $Mg_{0.1}Fe_{0.9}O$, was proposed as a carrier of the 19.5 μm feature which is accompanied by 13 and 17 μm features of oxygen-rich stars (Posch et al. 2002). Authors suggested the existence of a shell dominated by oxide dusts not accompanied by silicate dust around the circumstellar space. This implies that oxides formed under different physical condition from amorphous silicate dust.

In the present work, we focus on the dust analog which emits Sil-like spectrum. Our synthesized material MS-3 shows a Sil-like spectrum, although our spectrum was obtained by RAIRS. Gail & Sedlmayr (1999) discussed processes of dust formation around an M star. They reported that olivine, periclase (MgO), and a small fraction of quartz (SiO_2) are formed in the outflow. Kozasa & Sogawa (1997, 1998) and Sogawa & Kozasa (1999) calculated the condensation temperature and crystallized volume fraction of silicate dust formation of a typical aged star with and without Al_2O_3 as a function of distance for a given mass-loss rate. Their results show that the condensation temperature without nuclei is ranging from ~ 900 K (mass-loss rate = $4 \times 10^{-5} M_\odot/yr$) to ~ 400 K (mass-loss rate = $1 \times 10^{-6} M_\odot/yr$).

Onaka et al. (2002) observed the infrared spectrum of Z Cyg over an entire light cycle. The object is an oxygen-rich Mira variable star. The infrared spectral features indicate that the dust is amorphous during the light cycle. However, ratios of the peak height of 10 to the 18 μm changes during a light cycle. They attributed it to a change of dust-temperature and they estimated the highest dust temperature to be 700 ± 100 K. Simpson (1991) also assumed the temperature of inner dust

shell is in the range 400–800 K. The dust formation in these objects occurred at a lower temperature than those assumed previously.

The chemical composition (metal composition), oxidation degree (the ratio of oxygen to metals), mineral compositions, amorphous or crystalline, have been discussed regarding dust formation. Oxygen-deficient materials have been proposed as a candidate material. Nuth & Donn (1983) made condensates from SiO and Mg in ambient H₂ and Suzuki et al. (2000) made a condensate from SiO and Mg or Fe gas under vacuum. We have made a SiO-condensate in vacuum and discussed its infrared feature (Wada et al. 1991). We think that dusts in circumstellar spaces have various degrees of oxidation.

In the present work, we synthesized dust analogs in an O₂ atmosphere. Silicates, oxides, silicide, silicon are found to be possible products. At about 650 K, an amorphous silicate was formed from vapors of SiO and Mg in our experiments. Silicide was observed in the surface region of the products. The amorphous silicate was formed by oxidation-reduction reaction in O-deficient silicate (Mg₂SiO_{4-x}, MgSiO_{3-x}). On the other hand, oxides were main products on a cold substrate whose temperature was lower than 650 K. However, as oxidation did not proceed sufficiently, the product contained SiO_x and metallic Mg. Our experiments indicate that temperature and ambient O₂ pressure are important factors as to whether the amorphous silicate forms or oxides form.

The net reaction of the Mg-silicate (olivine) is expressed as:
 $2\text{Mg} + \text{SiO} + 3\text{H}_2\text{O} \rightarrow \text{Mg}_2\text{SiO}_4(\text{olivine}) + 3\text{H}_2$.

This expression follows that of Ferrarotti & Gail (2001). However we removed Fe in the equation since we did not include Fe in our experiment for simplicity.

There are of course differences in our experiment and the dust formation in circumstellar space. As discussed above, oxidizing species in the circumstellar environment is different from O₂, for example, H₂O, atomic oxygen, and OH radical. Therefore, the concentration of oxygen in the products would differ from those obtained in our experiment.

At present we do not understand completely the chemical composition (Mg/Si/O) of our products and that of circumstellar dusts of evolved stars. Studies on the chemical composition and the chemical structure of the material and other pathways to silicate formation are future problems.

4. Summary

We studied the silicate formation mechanism experimentally. Our experiments indicate following.

1. With a substrate temperature under 650 K, oxides, MgO and SiO_x, are the main products.
2. At about 650 K, amorphous silicate is formed from vapors of Mg and SiO in O₂ atmosphere.
3. XPS showed that amorphous silicate formed by a chemical reaction of oxidation-reduction of O-deficient silicate.
4. It is suggested by our experiments that around oxygen-rich mass loss stars amorphous silicate is formed through O-deficient silicate when the dust temperature is about 650 K or higher.

Acknowledgements. Part of this work was supported by Grant-in-Aid for Scientific Research (B)(2) project number 11440063 from Japan Society for the Promotion of Science.

References

- An, K. S., Park, R. J., Kim, J. S., et al. 1995, *J. Appl. Phys.*, 78, 1151
 Barranco, A., Mejías, J. A., Espinós, J. P., et al. 2001, *J. Vac. Sci. Technol. A.*, 19, 136
 Begemann, B., Dorschner, J., Henning, Th., et al. 1997, *ApJ*, 476, 199
 Brucato, J. R., Colangeli, L. Mennella, V., et al. 1999, *A&A*, 348, 1012
 Day, K. L. 1979, *Ap&SS*, 65, 173
 Dorschner, J., Friedemann, C., Gürtler, J., et al. 1986, *MNRAS*, 218, 37
 Dorschner, J., Begemann, B., Henning, Th., et al. 1995, *A&A*, 300, 503
 Fabian, D., Posch, Th., Mutschke, H., et al. 2001, *A&A*, 373, 1125
 Farmer, V. C. 1974, *The infrared spectra of minerals*, ed. V. C. Farmer (Mineralogical Society), 184
 Ferrarotti, A. S., & Gail, H.-P. 2001, *A&A*, 371, 133
 Gail, H. P., & Sedlmayr, E. 1999, *A&A*, 347, 594
 Golden, W. G. 1985, in *Fourier-Transform Infrared Spectroscopy*, ed. J. R. Ferraro, & L. J. Basile (Florida: Academic Press Inc.), 4, 315
 Guittet, M. J., Crocombette, J. P., & Gautier-Soyer, M. 2001, *Phys. Rev. B*, 63, 125117
 Jäger, C., Mutschke, H., Begemann, B., et al. 1994, *A&A*, 292, 641
 Kaito, C., Ojima, Y., Kido, O., et al. 2001, *M&PSA*, 36, A91
 Koike, C., & Tsuchiyama, A. 1992, *MNRAS*, 255, 248
 Kozasa, T., & Sogawa, H. 1997, *Ap&SS*, 251, 165
 Kozasa, T., & Sogawa, H. 1998, *Ap&SS*, 264, 654
 Little-Marenin, I. R., & Little, S. J. 1990, *AJ*, 99, 1173
 Miyata, T., Katata, H., Okamoto, Y., et al. 2000, *ApJ*, 531, 917
 Moreno, J. A., Garrido, B., Samitier, J., et al. 1997, *J. Appl. Phys.*, 81, 1933
 Nakamura, M., Mochizuki, Y., Usami, K., et al. 1984, *Solid State Comm.*, 50, 1079
 Nuth, J. A., & Donn, B. 1983, *J. Geophys. Res. Suppl.*, 88, A847
 Onaka, T., de Jong, T., & Willems, F. J. 1989, *A&A*, 218, 169
 Onaka, T., de Jong, T., & Yamamura, I. 2002, *A&A*, 388, 573
 Posch, Th., Kerschbaum, F., Mutschke, H., et al. 2002, *A&A*, 393, L7
 Rietmeijer, F. J. M., Nuth III, J. A., & Karner, J. M. 1999, *ApJ*, 527, 395
 Simpson, J. P. 1991, *ApJ*, 368, 570
 Sogawa, H., & Kozasa, T. 1999, *ApJ*, 516, L33
 Speck, A. K., Barlow, M. J., Sylvester, R. J., et al. 2000, *A&AS*, 147, 437
 Stephens, J. R., & Russell, R. W. 1979, *ApJ*, 228, 780
 Suzuki, N., Kimura, S., Nakada, T., et al. 2000, *Meteoritics & Planetary Sci.*, 35, 1269
 Trchová, M., Zemek, J., & Jurek, K. 1998, *J. Appl. Phys.*, 82, 3519
 Wada, S., Sakata, A., & Tokunaga, A. T. 1991, *ApJ*, 375, L17